Geophysical Research Letters

RESEARCH LETTER
10.1029/2020GL088897

Critical Zone Storage Controls on the Water Ages of Ecohydrological Outputs

S. Kuppel[1,2,3], D. Tetzlaff[4,5,3], M. P. Maneta[6], and C. Soulsby[3,4]

[1]Institut de Physique du Globe de Paris, CNRS - University of Paris, Paris, France, [2]INRAE, RiverLy, Villeurbanne, France, [3]Northern Rivers Institute, University of Aberdeen, Aberdeen, UK, [4]Leibniz Institute of Freshwater Ecology and Inland Fisheries, Berlin, Germany, [5]Department of Geography, Humboldt University Berlin, Berlin, Germany, [6]Geosciences Department, University of Montana, Missoula, MT, USA

Key Points:
- Age since precipitation displays inverse storage effect in stream, but not transpiration and soil evaporation, in a humid northern catchment
- Hysteresis between storage and the age of transpired water suggests cross-season carryover, despite weak hydroclimatic seasonality
- Downslope water subsidies result in valley bottom having weaker storage-age relationships than seen in freely draining hillslopes

Supporting Information:
- Supporting Information S1

Correspondence to:
D. Tetzlaff,
d.tetzlaff@igb-berlin.de

Citation:
Kuppel, S., Tetzlaff, D., Maneta, M. P., & Soulsby, C. (2020). Critical zone storage controls on the water ages of ecohydrological outputs. *Geophysical Research Letters*, *47*, e2020GL088897. https://doi.org/10.1029/2020GL088897

Received 15 MAY 2020
Accepted 12 JUL 2020
Accepted article online 17 JUL 2020
Corrected 15 SEP 2020

[Correction added on 15 SEP 2020, after first online publication: Projekt Deal funding statement has been added.]

Abstract Spatially explicit knowledge of the origins of water resources for ecosystems and rivers is challenging when using tracer data alone. We use simulations from a spatially distributed model calibrated by extensive ecohydrological data sets in a small, energy-limited catchment, where hillslope-riparian dynamics are broadly representative of humid boreal headwater catchments that are experiencing rapid environmental transition. We hypothesize that in addition to wetness status, landscape heterogeneity modulates the water pathways that sustain ecosystem function and streamflows. Simulations show that catchment storage inversely controls stream water ages year-round, but only during the drier seasons for transpiration and soil evaporation. The ages of these evaporative outputs depend much less on wetness status in the oft-saturated riparian soils than on the freely draining hillslopes that subsidize them. This work highlights the need to consider local dynamics and time-changing lateral heterogeneities when interpreting the ages, and thus the vulnerability, of water resources feeding streams and ecosystems in landscapes.

Plain Language Summary Knowing how much time water spends in a landscape (its "age") helps understanding how water travels through it. These dynamics inform of the stability of water resources for ecosystems and societies, and of their vulnerabilities under climate and land use changes. Water ages may vary depending on how wet or dry a location gets between seasons and years. We thus need to learn more about the demographics ("how much and how old?") of the water used by plants, evaporated from soils, and flowing in streams, but it is often impossible to monitor the heterogeneity of water pathways within landscapes. Addressing this challenge, we used a numerical model built upon coupling ecohydrological processes and that maps landscape locations. We adjusted this model using multiple data sets in a catchment representative of humid boreal environments where climate and vegetation are rapidly changing. We found markedly different aging patterns between water escaping the system through the plants, soils, and stream, depending on water storage status. This changing duration of water movement also differs between the catchment as a whole and its parts. This method can be used to better understand the multiple ways in which water moves through landscapes, in current and future conditions.

1. Introduction

The age of water as it is routed along different pathways within a landscape, that is, the transit time to exit from entry as zero-aged inputs (e.g., precipitation in catchment hydrology or groundwater recharge in hydrogeology), has long been recognized as an important metric that explicitly indexes linkages between stores and fluxes (Bolin & Rodhe, 1973; Hrachowitz et al., 2016). In particular, the demographics of the water ultimately used by vegetation or evaporated from the soil directly informs on the "temporal depth" of the resources supporting life and the biogeochemical cycles in the shallow underground of the critical zone (Sprenger et al., 2019). From seasonal carryover of precipitation inputs (Allen et al., 2019; Kuppel et al., 2017) to vegetation responses to interannual variations in water availability (Bales et al., 2018; Chitra-Tarak et al., 2018; Hahm et al., 2019), knowing the ages of this "green water" (i.e., not feeding streamflow nor deep recharge; Falkenmark & Rockström, 2006) would crucially help in assessing the vulnerability of natural vegetation communities to drought and climatic stress and the sustainability of managed systems (e.g., timber and rain-fed agrosystems).

Quantifying the demographics of green water has however received little attention (Soulsby, Birkel, et al., 2016), due to the difficulty of directly disentangling the components of green water dynamics outside of carefully controlled experiments (Evaristo et al., 2019). Most of the analytical developments regarding transit time characterization have remained focused on dating stream water or groundwater using concentrations in environmental tracers (Bethke & Johnson, 2008; McGuire & McDonnell, 2015), for which advanced analytical frameworks resolve the water age distribution of outputs or of water stores, sometimes linking the two (Benettin et al., 2013; Botter, 2012; Harman, 2015, 2019; Hrachowitz et al., 2013; Jasechko, 2019; Jasechko et al., 2016; Rinaldo et al., 2015; Rodriguez & Klaus, 2019). These efforts have highlighted the dynamic link between storage dynamics and water ages in streamflow as a key signature of hydrological functioning, yet there is currently no framework to assess how such relationships would translate for spatially distributed outputs such as plant transpiration and soil evaporation. In most cases water ages are interpreted as a mixture of water being partitioned between shallower and deeper flow paths (e.g., surface runoff, interflow, and groundwater lateral flow) in a lumped description of the spatial domain. This vertical view, however, remains to be articulated with the lateral heterogeneity in critical zone attributes (e.g., land cover type, topographic position, subsurface properties, vegetation phenology, and slope exposure) and resulting variability of pathways, mixing, and storages. This will help not only avoiding misinterpretation of apparent water ages dynamics at spatially aggregated scales (Kirchner, 2016; Soulsby et al., 2015) but also, crucially, better capturing heterogeneous ecohydrological responses to environmental changes observed within real-world landscapes (Bales et al., 2018).

Addressing the important issue of water availability in the critical zone will significantly benefit from using the wealth of information from ecohydrological measurements of water composition, fluxes, and stores to constrain process-based models, as these then inform about internal hydrological states (Maneta et al., 2018; Wilusz et al., 2020; Yang et al., 2018). We do so using a novel spatially distributed model where the time-varying water ages in ecohydrological fluxes are dynamically derived from mixing equations at the grid cell level. It is applied in a small (3.2 km^2) energy-limited, humid headwater catchment where the model has been previously calibrated and validated using exceptionally diverse and long-term data sets (Kuppel et al., 2018a, 2018b). The present analysis tests how ubiquitous is an inverse storage effect across critical zone water outputs. We go beyond previous studies by examining how seasonal storage-age relationships in catchment subunits contribute to the catchment-scale patterns, addressing the following questions: (1) How dependent on spatial scale and location are the relationships between the wetness state and the ages of water transpired by the plants, evaporated from the soil, and flowing in the stream? (2) What is the contribution of time-variable lateral heterogeneity to the seasonal variability of catchment-level water output ages? We highlight the strong control of landscape heterogeneity on the relative importance of flow paths that contribute water for ecosystem health and streamflow generation. These findings thus advance our understanding of the vulnerability of ecosystem water supplies to precipitation variability and land cover change.

2. Materials and Methods

2.1. Study Catchment

Bruntland Burn is a 3.2 km^2 headwater catchment in the Scottish Highlands (Figure S1). Elevation ranges between 220 and 560 m above sea level, with a wide valley bottom and steep slopes, typical of postglacial landscapes. The bedrock (mainly granite and meta-sediments) underlies glacial drift deposits that cover 60–70% of the catchment and maintain a perennial source of base flow to the stream (Soulsby, Bradford, et al., 2016). These deposits are overlain by ~1 m deep histosols (peats and peaty gleys) in the riparian area (~21% of the catchment area). The remainder (~79%) of the catchment pedology is dominated by freely draining podzols (<0.7 m deep) on the hillslopes, while thin regosols (rankers) are found where drift deposits are marginal (above 400 masl). Spatial patterns of land cover reflect these hydropedological units. Heather shrublands (*Calluna vulgaris* and *Erica* spp.) and Scots pine (*Pinus sylvestris L.*) are the dominant vegetation over the hillslopes. The former is secondary vegetation following deforestation and subsequent overgrazing by red deer (*Cervus elaphus*) and sheep, while Scots pine forest would be the natural vegetation cover, now restricted to steeper inaccessible hillslopes and fenced plantations. Finally, grasses (*Molinia caerulea*) cover the riparian gley soils, while the peat is dominated by bog

mosses (*Sphagnum* spp.). The water balance is energy limited; annual precipitation is ~1,000 mm with a slight winter maximum, about 400 mm becomes evapotranspiration (ET) with pronounced seasonality (Birkel et al., 2011). Mean annual temperature is 7°C, and monthly-averaged temperatures remain above 0°C; the climate is temperate to boreal oceanic; <5% of precipitation usually occurs as snowfall.

2.2. Critical Zone Ecohydrological Model

We used EcH$_2$O-iso, a process-based, fully distributed ecohydrological model designed to jointly simulate energy, water, and vegetation dynamics in the critical zone (Kuppel et al., 2018a). EcH$_2$O-iso couples a two-layer energy balance scheme based on flux-gradient similarity (separately computing transpiration, evaporation of intercepted water, and soil evaporation), a hydrological module for vertical and lateral transfers (using a 1-D kinematic wave approximation for stream and groundwater), and a biomass component to simulate vegetation phenology and growth (Maneta & Silverman, 2013). Root water uptake profile uses a parameterized exponential form across the three layers of the hydrological domain (encompassing the vadose zone and groundwater), and soil evaporation is restricted to the top layer. EcH$_2$O-iso tracks stable isotopes (^{2}H and ^{18}O) ratios in water and water ages. For each pixel and critical zone compartment, a full-mixing mass balance equation is applied to signatures (isotopic ratios and ages) at each sub-time step when water is exchanged (and includes evaporative fractionation of isotopes), providing a time-varying mean value (Kuppel et al., 2018a). Because outgoing fluxes have the same fully mixed signature as their feeding pool(s), the mean water ages (MWAs) in the former locally equates the water ages in the latter. More details on EcH$_2$O-iso, and recent developments, can be found in Smith et al. (2019). The model was run at daily time steps using a 100×100 m^2 grid, from February 2013 to February 2016 (see section 2.3 and the supporting information).

2.3. Data Sets and Model Calibration

The model has been extensively calibrated using a wide range of data sets (Kuppel et al., 2018a, 2018b). Calibration data include stream discharge at the outlet, soil water content (five sites, multiple depths), sapflow-derived pine stand transpiration (two sites), top-of-canopy net radiation (three sites), and isotope ratios (δ^2H and δ^{18}O) at the stream outlet, in bulk soil water (four sites), and groundwater (four wells), as summarized in Table S1 and in Kuppel et al. (2018a, 2018b). Thirty simulations were selected by combining the cumulative distribution functions of the goodness of fit to each calibration data set (Table S1), from the 150,000 parameters configurations initially sampled (further details in Kuppel et al., 2018a, 2018b). This ensemble of "best runs" satisfactorily captured catchment behavior in terms of water fluxes, stores, and velocity (Figure S2). A 12-year spinup period was used during calibration to limit transient effects in the different stores, fluxes, and isotopic composition. These ensemble simulations were then rerun with a 30-year spinup, given the longer period necessary for water ages to stabilize (Figure S3).

2.4. Analysis

We exclude canopy-intercepted water from our analysis of water fluxes, stores, and age dynamics. EcH$_2$O-iso does not simulate stemflow, so intercepted water does not mix with the below-canopy compartments; there is field-based evidence that it is a reasonable simplification as stemflow accounts for <1% of net precipitation here (Soulsby et al., 2017). We acknowledge that evaporation of intercepted water makes up a substantial part of evapotranspiration (ET), associated to very young ages (~38 ± 13% of annual ET and aged a few days, not shown). In the remainder of this study, precipitation inputs are adjusted for interception losses (effective precipitation; Figure 1a). Finally, our analysis utilizes the normalization proposed by (Zuecco et al., 2016), using the maximum and minimum values for each model realization:

$$x^*(t) = \frac{x(t) - min(x)}{max(x) - min(x)}, \quad (1)$$

where x is either water age or storage. This allows focusing on the intrasimulation seasonal dynamics for each of the catchment parameterizations in the ensemble approach adopted here, removing intermodel dispersion arising from different initial conditions after spinup.

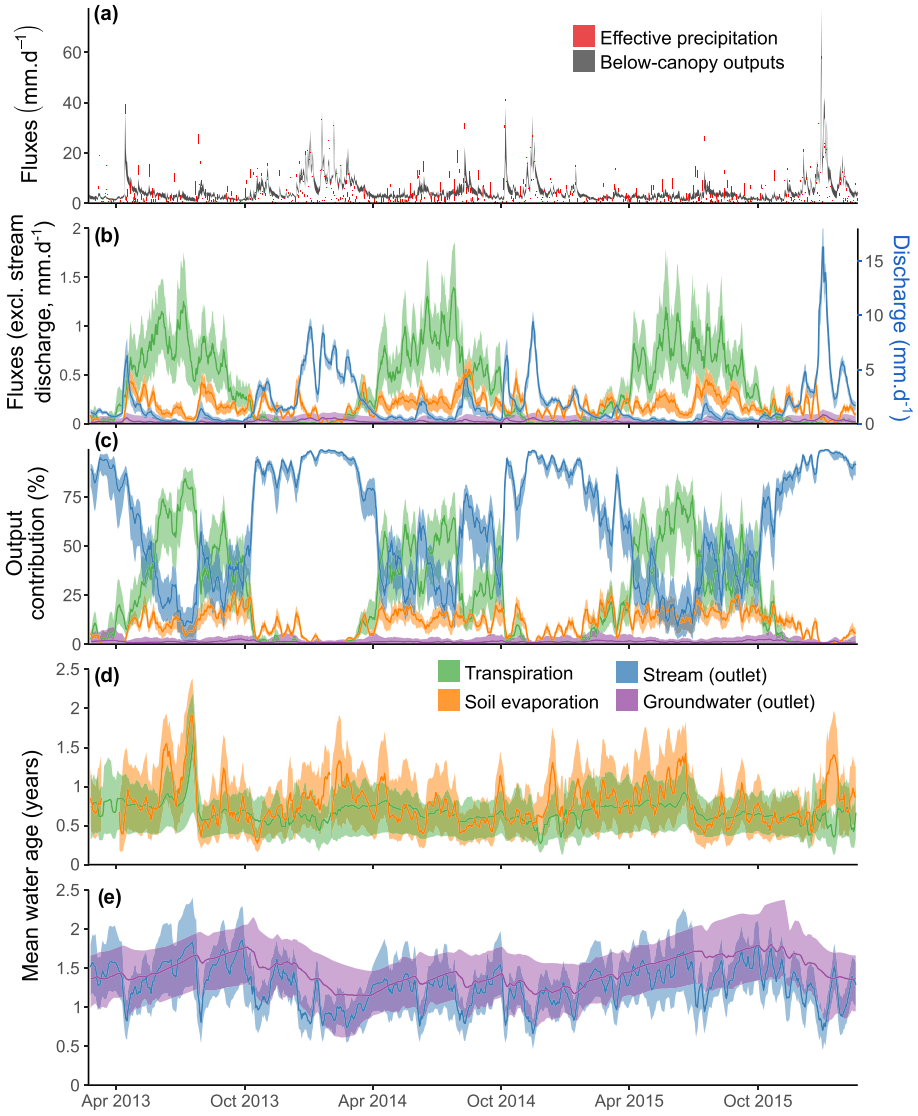

Figure 1. (a) Catchment-scale time series of the daily below-canopy water budget at Bruntland Burn. Below-canopy outputs are decomposed into ecohydrological components—note the right *y* axis for stream discharge—(b) showing their relative contributions (c) and mean water ages (d, e). The 80% intervals (errors bars and ribbons) are shown, along with ensemble medians and an additional 7-day smoothing in (b–e), to improve readability.

3. Results

3.1. Catchment Storage and Water Ages

The below-canopy catchment budget is dominated by stream discharge (Figure 1b), yet the relative contribution of soil evaporation and transpiration is dominant during the growing season (Figure 1c). A large predictive uncertainty surrounds the age of groundwater outputs (Figure 1d); however, this flux remains small in all ensemble simulations. As a result, we do not analyze the patterns of lateral groundwater outflow and limit our focus to the dynamics of soil evaporation, plant transpiration, and stream outflow.

The MWAs in stream water and transpiration clearly exhibit an inverse storage relationship—that is, water age since precipitation input decreases as catchment storage (including the unsaturated and saturated profile) increases, sensu (Harman, 2015)—across the simulation ensemble (Figures 2a and 2c). However, this inverse relationship is only found during the growing season for soil evaporation, while water age time tends to increase in winter time when this flux is small (Figure 2b). Some anticlockwise hysteresis is also clearly

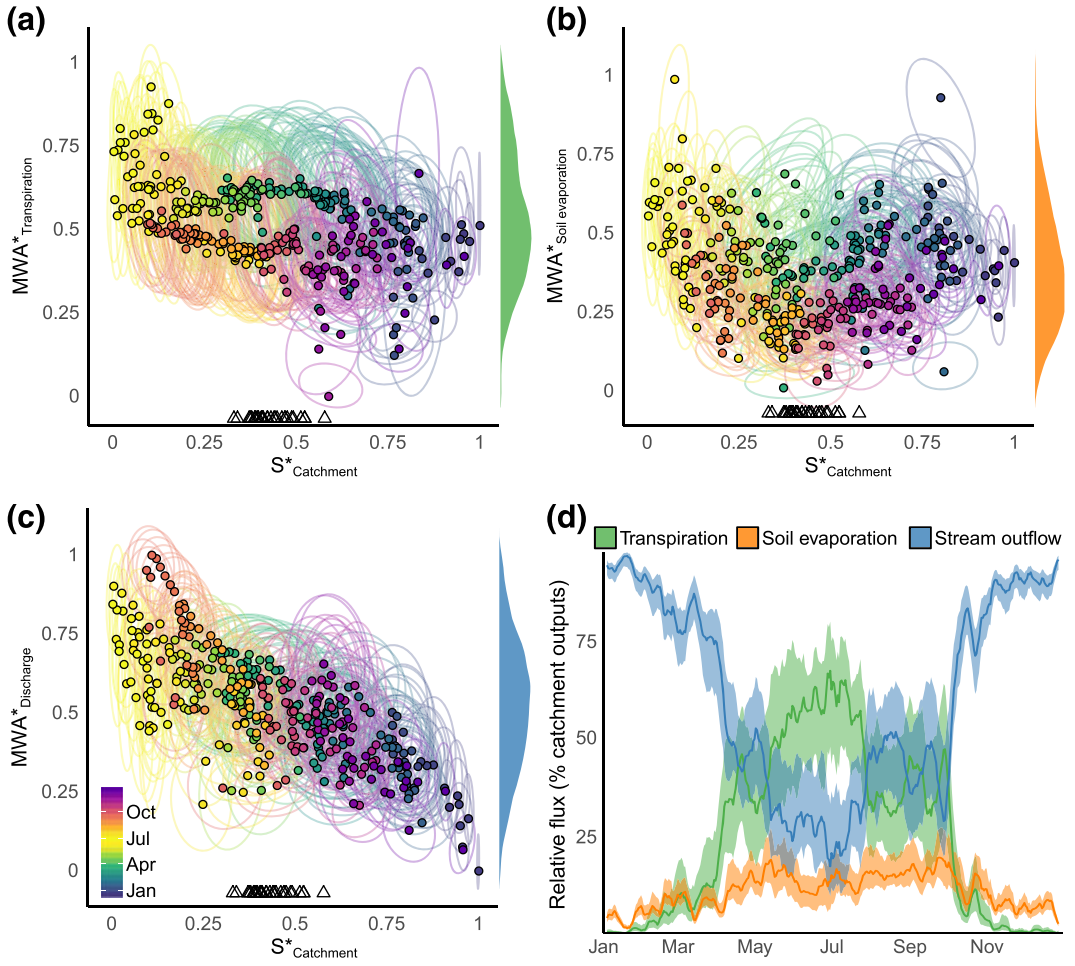

Figure 2. (a–c) Catchment-scale plots of normalized mean water ages (MWA*) in plant transpiration (a), soil evaporation (b), and outlet stream discharge (c) versus normalized catchment storage ($S^*_{catchment}$). Multiyear (2013–2016) daily means (color scale) are shown using cross-ensemble medians (small points) and 50% confidence ellipses. Open triangles indicate the median S*catchment for each simulation. (d) Mean seasonal cycle of each flux contribution to the below-canopy outputs (80% interval across the simulation ensemble).

visible for transpiration, and to a lesser extent soil evaporation (Figures 2a and 2b), meaning that for a similar storage value, these outgoing fluxes tap older water during the drying period (February to July) than during the rewetting period (August to January).

3.2. Preference of Age Extraction

We also computed the ratio between the age of water losses and the age of the water being currently stored in the catchment. This exit age ratio, hereafter EAR, is indicative of the "preference" toward younger waters (Soulsby, Birkel, et al., 2016). In other words, EAR is the degree to which each output mobilizes the youngest stores or rapid catchment flow pathways (EAR tending to 0, hereby highlighting heterogeneities) to tapping across well-mixed, less variable stores (EAR tending to 1). We find that EAR values between 0.25 and 0.5 for both green water outputs (Figures 3a and 3b). We interpret the limited seasonal variations as a high synchronicity between catchment water demographics and that of extracted water, consistent with the full mixing assumptions used at grid cell level and the generally weak seasonality of catchment inputs and limited water stress in the catchment at any point of the year. By contrast, streamflow shows a preference for comparatively older water pools in the catchment, while a clear progression toward younger water extraction with increased wetness states (and high flow), then mobilizing waters half the age (or less) than those stored in the catchment.

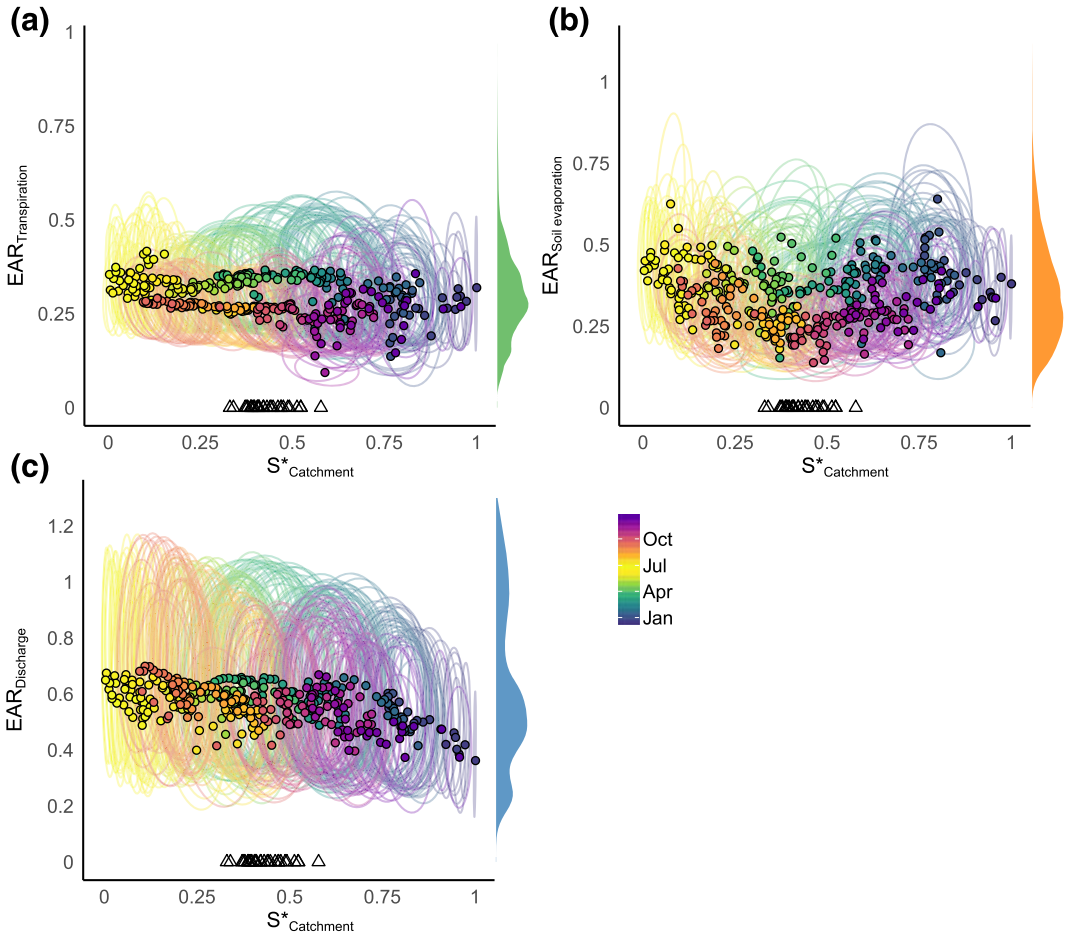

Figure 3. Catchment-scale plots of exit age ratio (EAR, the ratio between the age of water in outputs and that of water currently stored in the critical zone) of plant transpiration (a), soil evaporation (b), and outlet stream discharge **(c)** versus the normalized catchment storage ($S^*_{catchment}$). Multiyear (2013–2016) daily means (color scale) are shown using cross-ensemble medians (small points) and 50% confidence ellipses. Open triangles indicate the median S*catchment for each simulation.

3.3. Dynamics in Dominant Hydropedological Units

The above description provides an integrated perspective at the catchment scale of the age demographics of water losses in the critical zone. However, we also seek to disentangle the interplay between local dynamics and the relative contributions in different hydropedological units. In general, a weaker control of storage on water ages is found in the valley bottom than on the hillslopes (Figures 4a–4d). In addition, the patterns for transpiration ages at the catchment scale (Figure 2a) mostly reflect those found on the hillslopes with an inverse storage effect and hysteresis (Figure 4a), related to the dominant contribution of Scots pine and heather shrubs transpiration covering ~80% of the catchment (in terms of spatially aggregated budget; Figure 4e). In the case of soil evaporation (Figures 4c and 4d), these individual units display less symmetrically V-shaped MWA* dynamics than found at the catchment scale (Figure 2a), with a more limited increase of winter ages on the hillslopes and noisier variations on the valley bottom. We note that these normalized seasonal dynamics are relative to a baseline of younger water evapotranspired in the hillslopes than in the valley bottom (<1 and 1–2.5 years, respectively; Figure S4).

4. Discussion

The time-variant nature of water ages from precipitation to output has been widely observed in various critical zone settings (Benettin et al., 2017; Destouni, 1991; Heidbüchel et al., 2012; Hrachowitz

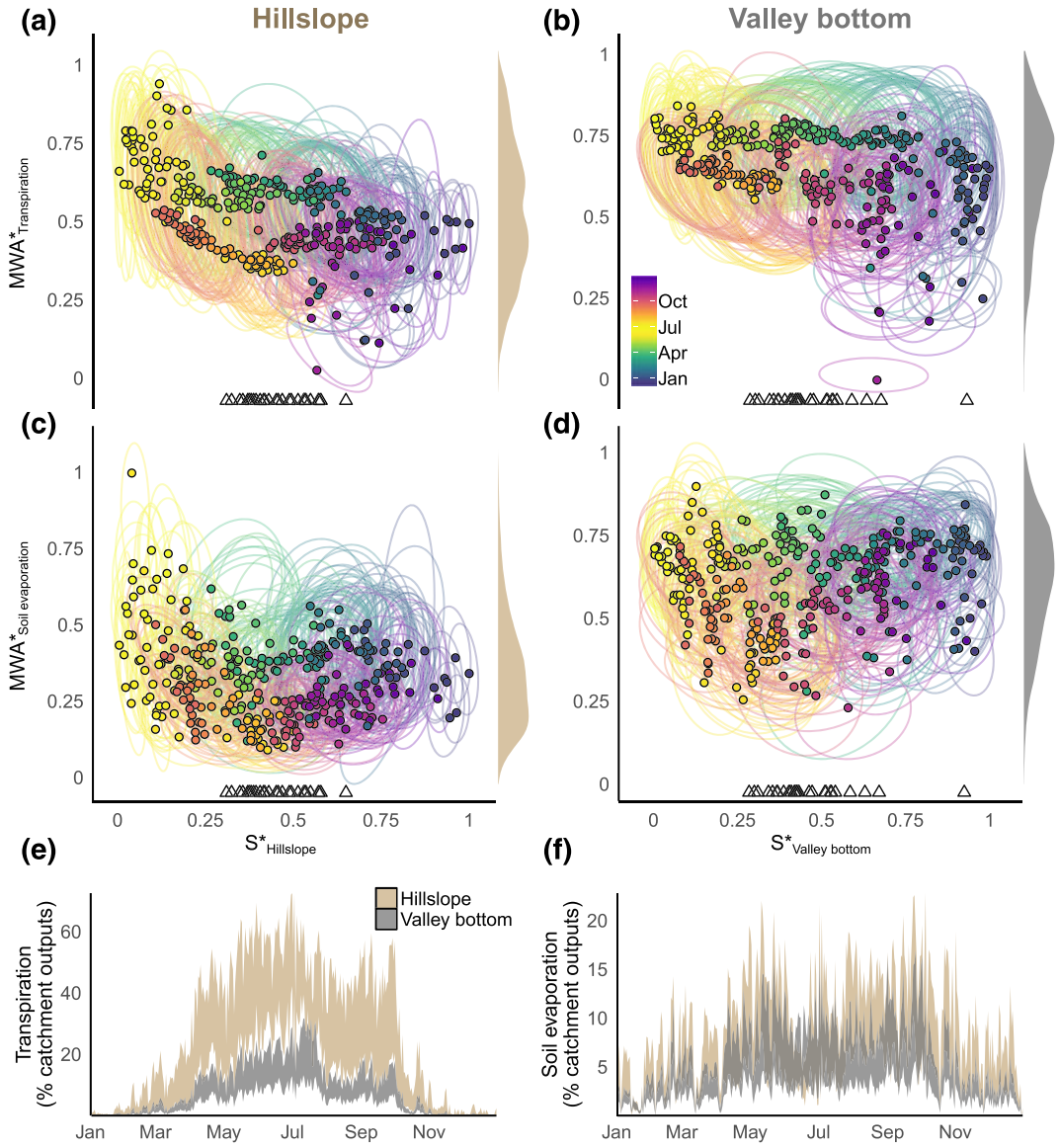

Figure 4. (a, b) Normalized mean water ages (MWA*) of transpiration against the normalized storage (S*) state of the subsurface, spatially aggregated over two subcatchment units: The hillslopes overlain by podzolic and ranker soils (a, ~80% of the area) and the valley bottom overlain by peat/peaty gley soils (b, ~20% of the area). (c, d) The same as (a) and (b) with the MWA* of soil evaporation. Multiyear (2013–2016) daily means (color scale) are shown using cross-ensemble medians (small points) and 50% confidence ellipses. Open triangles indicate the median S* for each simulation. **(e, f)** Mean seasonal cycle of the contributions of soil evaporation (e) and plant transpiration (f) to daily catchment-scale below-canopy budgets (80% interval across the simulation ensemble); note the difference of vertical scale between panels (e) and (f).

et al., 2015; van der Velde et al., 2012). Taking the example of a well-studied catchment, we show that while MWAs are generally controlled by storage, seasonal patterns are significantly different between the output fluxes and the spatial scales we considered (catchment and hydropedological subunits). In particular, our approach reveals that the "inverse storage effect" defined by Harman (2015) applies to stream water ages at the catchment scale but is not a ubiquitous feature across outputs and in subcatchment units.

Water ages in catchment-scale transpiration had a rapid and inverse response to storage variations particularly visible during the driest months, at the peak of the growing season. However, the bulk of seasonal dynamics exhibited a hysteretic storage-age behavior in which spring transpiration used older water than

in fall (by ~25% of the seasonal age range), despite similar catchment storage status (Figure 2a). This seems to point to a seasonal carryover of winter rewetting events that partially subsidize spring transpiration, while plant water use in fall relies on more recently infiltrated precipitation after summer drying. Such an asymmetrical buffering effect was less identifiable for soil evaporation where it might be obscured by short-term variability (Figure 2b), probably owing to the fact that topsoil dynamics are more responsive to hydroclimate variability, and thus less prone to "memory effects," than the deeper layers accessible to the root water uptake. In addition, the distinctively V-shaped seasonal storage-age relationship of soil evaporation indicates the fundamentally different dynamics between the two components of evaporative losses, even at the aggregated scale first considered here, thereby pointing at the limits of only considering a single evapotranspiration term to conceptualize ecohydrological couplings driving partitioning and water budget in catchments (Fatichi et al., 2012, 2014; Vivoni, 2012). Finally, only MWAs in streamflow displayed a consistent inverse storage effect (Figure 2c), a feature observed in various settings (e.g., Harman, 2015; Pangle et al., 2017; Rodriguez et al., 2018), including the one studied here with independent approaches (Benettin et al., 2017). The synchronous decrease in the ratio of stream water ages to catchment-stored water ages (Figure 3c) reflects an increasing relative contribution of recent, less-well-mixed water to the stream in wetter conditions (Harman, 2019). In other words, during the rewetting period (August to January), stream-feeding pathways increasingly bypass and outpace contribution of older, mixed water in deeper catchment stores. The associated seasonal decrease of transit times (since lateral and precipitation inputs) in the valley bottom, but also on the hillslopes in the wettest months (Figure S5c), is consistent with the reported increase in extent of surface connectivity via saturation overland flow, first in the saturated riparian histosols and eventually including the hillslope podzols (Tetzlaff et al., 2014).

In the valley bottom, the weak seasonal variability of water ages (and in particular the lack of water ages increase in summer; Figure 4) and markedly older baseline ages than the hillslopes (Figure S4) translated the generally wet conditions in the riparian area, which acts as a hydrological buffer (McGlynn & Seibert, 2003; Tetzlaff et al., 2014). This downslope water subsidy maintained leveled soil evaporation rate throughout the months when storage was lowest (Figures 4f and S4e) and is consistent with our estimate of slow-draining lateral water fluxes from the hillslope with downslope transit time of about 6 months and even slower turnover within the valley bottom with 1–2 year transit times (Figures S5a and S5b). The stronger (and generally inverse) constraint of storage on MWA on the hillslope reflected the higher turnover in these shallower, freely-draining podzols (Sprenger et al., 2018), where the limited hydroclimatic seasonality makes green water demographics more controlled by the atmospheric demand.

These differences between subcatchment units draw attention to the interplay between local dynamics of water ages and spatial organization of contributing fluxes, whereby a range of catchment age dynamics that could be interpreted as complex mixing patterns may also be produced by time-changing lateral heterogeneity. Using the daily fraction of catchment transpiration and soil evaporation budgets taking place on the hillslope as indices of such an heterogeneity, we found that landscape organization explains around half of the catchment-scale, seasonal variability of the ages of these two green water outputs ($43 \pm 25\%$ and $53 \pm 20\%$ across ensemble simulations, respectively, not shown). Although our numerical model uses full local mixing in each simulated compartment for each pixel, our spatially aggregated analyses of storage and water ages essentially describe a partially mixed system with changing macroscale water pathways over time. Our approach thus provides an alternative to catchment-lumped analytical formulations of time-variant transit time distributions (TTDs) and StorAge selection (SAS) functions and to numerical experiments testing the impact of partially mixing flows on water ages (e.g., Cain et al., 2019; Knighton et al., 2017). All provide different perspectives on how to model the unavoidable structural and functional heterogeneity of real-world catchments (Sprenger et al., 2019), but spatially-lumped descriptions cannot fully reject the full mixing hypothesis if a complex age response can also be reproduced with spatial heterogeneity, as is the case here.

There is thus a need to assess the relative importance of preferential flows at the pore scale (Beven & Germann, 2013) and areal scales (i.e., spatial organization; Hendrickx & Flury, 2001) in the resulting catchment functioning. Our approach was limited to considering uniform flows in three hydrological layers of each grid cell, and our soil evaporation ages from a well-mixed topsoil likely underestimated the contribution of recent surface waters to this flux. Yet combining these simplified formulations with spatially distributed flow paths has allowed capturing water flux and tracer concentrations measured at multiple locations in several critical zone compartments of high-latitude catchments (Kuppel et al., 2018a; Smith et al., 2019).

In addition, accounting for local preferential flow may not always improve catchment-scale simulations (Glaser et al., 2019; Hopp et al., 2020). The present simulations further suggest that plants access relatively old water pools (from ~6 months on the hillslopes to >2 years in the valley bottom; Figure S4) with an hysteretic relationship to storage not found in streamflow ages. This modeling approach is therefore relevant to analyzing water flow paths as trajectories with spatially varying velocities, resulting in transient storage, connectivity, and changing heterogeneity (vertical and lateral) in catchment fluxes. In this framework, confronting simulated tracer concentrations to measurements at multiple locations in the critical zone (Penna et al., 2018) will help evaluate whether the proposed ecohydrological separation (Brooks et al., 2010) can be fully explained via the conservation of water masses in heterogeneously conducting media (Berghuijs & Allen, 2019) or further requires accounting for preferential pore space selection during root uptake (Sprenger & Allen, 2020).

The generic nature of hillslope-riparian couplings in real-world catchments makes our spatialized analysis relevant to identifying key contributing areas in the face of environmental changes. We show, for example, that the transit times from precipitation to lateral outputs in the hillslopes account for a third to half of streamflow ages at the outlet, suggesting high sensitivity of river flow to water partitioning on hillslopes. Yet the vast majority of catchment management solutions focus on riparian management (e.g., forest felling restrictions zones around streams or water quality buffer strips in agricultural land) as common-sense or cost-effective approaches, without often knowing the specific nature of hillslope-riparian interactions. These issues may be particularly crucial in high-latitude landscapes—such as the one studied here—where climate and land cover changes are inducing rapid shifts in snowfall/rainfall partition and vegetation cover. The presented ecohydrological modeling approach may help inferring the likely ecohydrological consequences of these changes, more critically so considering the general decline of high-latitude catchment monitoring (Laudon et al., 2017).

Data Availability Statement

The source code of the EcH$_2$O-iso model is publicly available on https://bitbucket.org/sylka/ech2o_iso/ (branch master_2.0). Input, forcing, and output files, along with scripts to launch ensemble simulations and create basic plots are on a Zenodo repository (doi: 10.5281/zenodo.3592491).

Acknowledgments

This work was supported by the European Research Council (ERC, project GA 335910 VeWa). M.P. Maneta acknowledges support from the NASA Ecological Forecasting Program Award #80NSSC19K00181 and NASA EPSCoR #80NSSC18M0025M. The authors are thankful to V. Ivanov, two anonymous reviewers, and E. Anguelova, whose comments and suggestions considerably improved the manuscript. Open access funding enabled and organized by Projekt DEAL.

References

Allen, S. T., Kirchner, J. W., Braun, S., Siegwolf, R. T., & Goldsmith, G. R. (2019). Seasonal origins of soil water used by trees. *Hydrology and Earth System Sciences*, *23*(2), 1199–1210. https://doi.org/10.5194/hess-23-1199-2019

Bales, R. C., Goulden, M. L., Hunsaker, C. T., Conklin, M. H., Hartsough, P. C., O'Geen, A. T., et al. (2018). Mechanisms controlling the impact of multi-year drought on mountain hydrology. *Scientific Reports*, *8*(1), 690–698. https://doi.org/10.1038/s41598-017-19007-0

Benettin, P., Soulsby, C., Birkel, C., Tetzlaff, D., Botter, G., & Rinaldo, A. (2017). Using SAS functions and high-resolution isotope data to unravel travel time distributions in headwater catchments. *Water Resources Research*, *53*, 1864–1878. https://doi.org/10.1002/2016WR020117

Benettin, P., Van Der Velde, Y., Van Der Zee, S. E., Rinaldo, A., & Botter, G. (2013). Chloride circulation in a lowland catchment and the formulation of transport by travel time distributions. *Water Resources Research*, *49*, 4619–4632. https://doi.org/10.1002/wrcr.20309

Berghuijs, W. R., & Allen, S. T. (2019). Waters flowing out of systems are younger than the waters stored in those same systems. *Hydrological Processes*, *33*(25), 3251–3254. https://doi.org/10.1002/hyp.13569

Bethke, C. M., & Johnson, T. M. (2008). Groundwater age and groundwater age dating. *Annual Review of Earth and Planetary Sciences*, *36*(1), 121–152. https://doi.org/10.1146/annurev.earth.36.031207.124210

Beven, K., & Germann, P. (2013). Macropores and water flow in soils revisited. *Water Resources Research*, *49*, 3071–3092. https://doi.org/10.1002/wrcr.20156

Birkel, C., Tetzlaff, D., Dunn, S. M., & Soulsby, C. (2011). Using time domain and geographic source tracers to conceptualize streamflow generation processes in lumped rainfall-runoff models. *Water Resources Research*, *47*, W02515. https://doi.org/10.1029/2010WR009547

Bolin, B., & Rodhe, H. (1973). A note on the concepts of age distribution and transit time in natural reservoirs. *Tellus*, *25*(1), 58–62. https://doi.org/10.1111/j.2153-3490.1973.tb01594.x

Botter, G. (2012). Catchment mixing processes and travel time distributions. *Water Resources Research*, *48*, W05545. https://doi.org/10.1029/2011WR011160

Brooks, J. R., Barnard, H. R., Coulombe, R., & McDonnell, J. J. (2010). Ecohydrologic separation of water between trees and streams in a Mediterranean climate. *Nature Geoscience*, *3*(2), 100–104. https://doi.org/10.1038/ngeo722

Cain, M. R., Ward, A. S., & Hrachowitz, M. (2019). Ecohydrologic separation alters interpreted hydrologic stores and fluxes in a headwater mountain catchment. *Hydrological Processes*, *33*(20), 2658–2675. https://doi.org/10.1002/hyp.13518

Chitra-Tarak, R., Ruiz, L., Dattaraja, H. S., Kumar, M. M., Riotte, J., Suresh, H. S., et al. (2018). The roots of the drought: Hydrology and water uptake strategies mediate forest-wide demographic response to precipitation. *Journal of Ecology*, *106*(4), 1495–1507. https://doi.org/10.1111/1365-2745.12925

Destouni, G. (1991). Applicability of the steady state flow assumption for solute advection in field soils. *Water Resources Research*, *27*(8), 2129–2140. https://doi.org/10.1029/91WR01115

Evaristo, J., Kim, M., van Haren, J., Pangle, L. A., Harman, C. J., Troch, P. A., & McDonnell, J. J. (2019). Characterizing the fluxes and age distribution of soil water, plant water, and deep percolation in a model tropical ecosystem. *Water Resources Research*, *55*, 3307–3327. https://doi.org/10.1029/2018WR023265

Falkenmark, M., & Rockström, J. (2006). The new blue and green water paradigm: Breaking new ground for water resources planning and management. *Journal of Water Resources Planning and Management*, *132*(3), 129–132. https://doi.org/10.1061/(ASCE)0733-9496(2006)132:3(129)

Fatichi, S., Ivanov, V. Y., & Caporali, E. (2012). A mechanistic ecohydrological model to investigate complex interactions in cold and warm water-controlled environments: 2. Spatiotemporal analyses. *Journal of Advances in Modeling Earth Systems*, *4*, M05003. https://doi.org/10.1029/2011MS000087

Fatichi, S., Zeeman, M. J., Fuhrer, J., & Burlando, P. (2014). Ecohydrological effects of management on subalpine grasslands: From local to catchment scale. *Water Resources Research*, *50*, 148–164. https://doi.org/10.1002/2013WR014535

Glaser, B., Jackisch, C., Hopp, L., & Klaus, J. (2019). How meaningful are plot-scale observations and simulations of preferential flow for catchment models? *Vadose Zone Journal*, *18*(1), 1–18. https://doi.org/10.2136/vzj2018.08.0146

Hahm, W. J., Dralle, D. N., Rempe, D. M., Bryk, A. B., Thompson, S. E., Dawson, T. E., & Dietrich, W. E. (2019). Low subsurface water storage capacity relative to annual rainfall decouples Mediterranean plant productivity and water use from rainfall variability. *Geophysical Research Letters*, *46*, 6544–6553. https://doi.org/10.1029/2019GL083294

Harman, C. J. (2015). Time-variable transit time distributions and transport: Theory and application to storage-dependent transport of chloride in a watershed. *Water Resources Research*, *51*, 1–30. https://doi.org/10.1002/2014WR015707

Harman, C. J. (2019). Age-ranked storage-discharge relations: A unified description of spatially lumped flow and water age in hydrologic systems. *Water Resources Research*, *55*, 7143–7165. https://doi.org/10.1029/2017WR022304

Heidbüchel, I., Troch, P. A., Lyon, S. W., & Weiler, M. (2012). The master transit time distribution of variable flow systems. *Water Resources Research*, *48*, W06520. https://doi.org/10.1029/2011WR011293

Hendrickx, J. M., & Flury, M. (2001). Uniform and preferential flow mechanisms in the vadose zone. In *Conceptual Models of Flow and Transport in the Fractured Vadose Zone* (pp. 149–187). Washington, DC: National Academy Press.

Hopp, L., Glaser, B., Klaus, J., & Schramm, T. (2020). The relevance of preferential flow in catchment scale simulations: Calibrating a 3D dual-permeability model using DREAM. *Hydrological Processes*, *34*(5), 1237–1254. https://doi.org/10.1002/hyp.13672

Hrachowitz, M., Benettin, P., Van Breukelen, B. M., Fovet, O., Howden, N. J., Ruiz, L., et al. (2016). Transit times—The link between hydrology and water quality at the catchment scale. *Wiley Interdisciplinary Reviews Water*, *3*(5), 629–657. https://doi.org/10.1002/wat2.1155

Hrachowitz, M., Fovet, O., Ruiz, L., & Savenije, H. H. G. (2015). Transit time distributions, legacy contamination and variability in biogeochemical 1/fα scaling: How are hydrological response dynamics linked to water quality at the catchment scale? *Hydrological Processes*, *29*(25), 5241–5256. https://doi.org/10.1002/hyp.10546

Hrachowitz, M., Savenije, H., Bogaard, T. A., Soulsby, C., & Tetzlaff, D. (2013). What can flux tracking teach us about water age distribution patterns and their temporal dynamics? *Hydrology and Earth System Sciences*, *17*(2), 2013.

Jasechko, S. (2019). Global isotope hydrogeology—Review. *Reviews of Geophysics*, *57*, 835–965. https://doi.org/10.1029/2018RG000627

Jasechko, S., Kirchner, J. W., Welker, J. M., & McDonnell, J. J. (2016). Substantial proportion of global streamflow less than three months old. *Nature Geoscience*, *9*(2), 126–129. https://doi.org/10.1038/ngeo2636

Kirchner, J. W. (2016). Aggregation in environmental systems—Part 1: Seasonal tracer cycles quantify young water fractions, but not mean transit times, in spatially heterogeneous catchments. *Hydrology and Earth System Sciences*, *20*(1), 279–297. https://doi.org/10.5194/hess-20-279-2016

Knighton, J., Saia, S. M., Morris, C. K., Archiblad, J. A., & Walter, M. T. (2017). Ecohydrologic considerations for modeling of stable water isotopes in a small intermittent watershed. *Hydrological Processes*, *31*(13), 2438–2452. https://doi.org/10.1002/hyp.11194

Kuppel, S., Fan, Y., & Jobbágy, E. G. (2017). Seasonal hydrologic buffer on continents: Patterns, drivers and ecological benefits. *Advances in Water Resources*, *102*, 178–187. https://doi.org/10.1016/j.advwatres.2017.01.004

Kuppel, S., Tetzlaff, D., Maneta, M. P., & Soulsby, C. (2018a). EcH2O-iso 1.0: Water isotopes and age tracking in a process-based, distributed ecohydrological model. *Geoscientific Model Development*, *11*(7), 3045–3069. https://doi.org/10.5194/gmd-11-3045-2018

Kuppel, S., Tetzlaff, D., Maneta, M. P., & Soulsby, C. (2018b). What can we learn from multi-data calibration of a process-based ecohydrological model? *Environmental Modelling & Software*, *101*, 301–316. https://doi.org/10.1016/j.envsoft.2018.01.001

Laudon, H., Spence, C., Buttle, J., Carey, S. K., McDonnell, J. J., McNamara, J. P., et al. (2017). Save northern high-latitude catchments. *Nature Geoscience*, *10*(5), 324–325. https://doi.org/10.1038/ngeo2947

Maneta, M. P., & Silverman, N. L. (2013). A spatially distributed model to simulate water, energy, and vegetation dynamics using information from regional climate models. *Earth Interactions*, *17*(11), 1–44. https://doi.org/10.1175/2012EI000472.1

Maneta, M. P., Soulsby, C., Kuppel, S., & Tetzlaff, D. (2018). Conceptualizing catchment storage dynamics and nonlinearities. *Hydrological Processes*, *32*(21), 3299–3303.

McGlynn, B. L., & Seibert, J. (2003). Distributed assessment of contributing area and riparian buffering along stream networks. *Water Resources Research*, *39*(4), 1082. https://doi.org/10.1029/2002WR001521

McGuire, K. J., & McDonnell, J. J. (2015). Tracer advances in catchment hydrology. *Hydrological Processes*, *29*(25), 5135–5138. https://doi.org/10.1002/hyp.10740

Pangle, L. A., Kim, M., Cardoso, C., Lora, M., Meira Neto, A. A., Volkmann, T. H., et al. (2017). The mechanistic basis for storage-dependent age distributions of water discharged from an experimental hillslope. *Water Resources Research*, *53*, 2733–2754. https://doi.org/10.1002/2016WR019901

Penna, D., Hopp, L., Scandellari, F., Allen, S. T., Benettin, P., Beyer, M., et al. (2018). Ideas and perspectives: Tracing terrestrial ecosystem water fluxes using hydrogen and oxygen stable isotopes—Challenges and opportunities from an interdisciplinary perspective. *Biogeosciences*, *15*(21), 6399–6415. https://doi.org/10.5194/bg-15-6399-2018

Rinaldo, A., Benettin, P., Harman, C. J., Hrachowitz, M., McGuire, K. J., Van Der Velde, Y., et al. (2015). Storage selection functions: A coherent framework for quantifying how catchments store and release water and solutes. *Water Resources Research*, *51*, 4840–4847. https://doi.org/10.1002/2015WR017273

Rodriguez, N. B., & Klaus, J. (2019). Catchment travel times from composite StorAge Selection functions representing the superposition of Streamflow generation processes. *Water Resources Research*, *55*, 9292–9314. https://doi.org/10.1029/2019WR024973

Rodriguez, N. B., McGuire, K. J., & Klaus, J. (2018). Time-varying storage–Water age relationships in a catchment with a Mediterranean climate. *Water Resources Research*, *54*, 3988–4008. https://doi.org/10.1029/2017WR021964

Smith, A., Tetzlaff, D., Laudon, H., Maneta, M., & Soulsby, C. (2019). Assessing the influence of soil freeze-thaw cycles on catchment water storage-flux-age interactions using a tracer-aided ecohydrological model. *Hydrology and Earth System Sciences*, *23*(8), 3319–3334. https://doi.org/10.5194/hess-23-3319-2019

Soulsby, C., Birkel, C., Geris, J., Dick, J., Tunaley, C., & Tetzlaff, D. (2015). Stream water age distributions controlled by storage dynamics and nonlinear hydrologic connectivity: Modeling with high-resolution isotope data. *Water Resources Research*, *51*, 7759–7776. https://doi.org/10.1002/2015WR017888

Soulsby, C., Birkel, C., & Tetzlaff, D. (2016). Characterizing the age distribution of catchment evaporative losses. *Hydrological Processes*, *30*(8), 1308–1312. https://doi.org/10.1002/hyp.10751

Soulsby, C., Bradford, J., Dick, J., McNamara, J. P., Geris, J., Lessels, J., et al. (2016). Using geophysical surveys to test tracer-based storage estimates in headwater catchments. *Hydrological Processes*, *30*(23), 4434–4445.

Soulsby, C., Braun, H., Sprenger, M., Weiler, M., & Tetzlaff, D. (2017). Influence of forest and shrub canopies on precipitation partitioning and isotopic signatures. *Hydrological Processes*, *31*(24), 4282–4296. https://doi.org/10.1002/hyp.11351

Sprenger, M., & Allen, S. T. (2020). Commentary: What ecohydrologic separation is and where we can go with it. *Water Resources Research*, *56*, e2020WR027238. https://doi.org/10.1029/2020WR027238

Sprenger, M., Stumpp, C., Weiler, M., Aeschbach, W., Allen, S. T., Benettin, P., et al. (2019). The demographics of water: A review of water ages in the critical zone. *Reviews of Geophysics*, *57*, 800–834. https://doi.org/10.1029/2018RG000633

Sprenger, M., Tetzlaff, D., Buttle, J., Laudon, H., & Soulsby, C. (2018). Water ages in the critical zone of long-term experimental sites in northern latitudes. *Hydrology and Earth System Sciences*, *22*(7), 3965–3981. https://doi.org/10.5194/hess-22-3965-2018

Tetzlaff, D., Birkel, C., Dick, J., Geris, J., & Soulsby, C. (2014). Storage dynamics in hydropedological units control hillslope connectivity, runoff generation, and the evolution of catchment transit time distributions. *Water Resources Research*, *50*, 969–985. https://doi.org/10.1002/2013WR014147

van der Velde, Y., Torfs, P. J. J. F., van der Zee, S. E. A. T. M., & Uijlenhoet, R. (2012). Quantifying catchment-scale mixing and its effect on time-varying travel time distributions. *Water Resources Research*, *48*, W06536. https://doi.org/10.1029/2011WR011310

Vivoni, E. R. (2012). Diagnosing seasonal vegetation impacts on evapotranspiration and its partitioning at the catchment scale during SMEX04–NAME. *Journal of Hydrometeorology*, *13*(5), 1631–1638. https://doi.org/10.1175/JHM-D-11-0131.1

Wilusz, D. C., Harman, C. J., Ball, W. B., Maxwell, R. M., & Buda, A. R. (2020). Using particle tracking to understand flow paths, age distributions, and the paradoxical origins of the inverse storage effect in an experimental catchment. *Water Resources Research*, *56*, e2019WR025140. https://doi.org/10.1029/2019WR025140

Yang, J., Heidbüchel, I., Musolff, A., Reinstorf, F., & Fleckenstein, J. H. (2018). Exploring the dynamics of transit times and subsurface mixing in a small agricultural catchment. *Water Resources Research*, *54*, 2317–2335. https://doi.org/10.1002/2017WR021896

Zuecco, G., Penna, D., Borga, M., & van Meerveld, H. J. (2016). A versatile index to characterize hysteresis between hydrological variables at the runoff event timescale. *Hydrological Processes*, *30*(9), 1449–1466. https://doi.org/10.1002/hyp.10681

References From the Supporting Information

Dee, D. P., Uppala, S. M., Simmons, A. J., Berrisford, P., Poli, P., Kobayashi, S., et al. (2011). The ERA-Interim reanalysis: Configuration and performance of the data assimilation system. *Quarterly Journal of the Royal Meteorological Society*, *137*(656), 553–597. https://doi.org/10.1002/qj.828

Met Office. (2017). Met Office Integrated Data Archive System (MIDAS) Land and Marine Surface Stations Data (1853–current). *NCAS British Atmospheric Data Centre*. Retrieved from http://catalogue.ceda.ac.uk/uuid/220a65615218d5c9cc9e4785a3234bd0